JURNAL KARTIKA KIMIA

J. Kartika Kimia, Mei 2026, 9, (1), 88-104
Journal homepage: http://jkk.unjani.ac.id/index.php/jkk
P-ISSN: 2655-1322 E-ISSN: 2655-0938

In Silico Investigation of EDTA-Functionalized ZSM-5 as a Rifampicin Drug Delivery System Against Tuberculosis-Related Targets

Indra Lasmana Tarigan[1,2,*], Nadia Rahmasari[1], Chairanisa Intan Kartika[1], Jonathan Sabar Simorangkir[1], Ailsa Putri Dyanti[1], Muhammad Irfan Nur Widad[1]
[1]Department of Chemistry, Faculty of Science and Technology, Universitas Jambi
[2]NPBC Laboratory, Faculty of Science and Technology, Universitas Jambi
*E-mail: indratarigan@unja.ac.id

DOI: https://doi.org/

Received: 19 Oct 2025, *Revised*: 27 May 2026, *Accepted*: 14 June 2026, *Online*: 18 June 2026

Abstract

Tuberculosis (TB) is a major infectious disease caused by Mycobacterium tuberculosis. Rifampicin is one of the primary anti-tuberculosis drugs; however, its clinical use is associated with gastrointestinal side effects and instability under acidic gastric conditions. Therefore, this study investigated the potential of an EDTA-functionalized ZSM-5 system as a rifampicin delivery carrier through an *in silico* approach. The study employed network pharmacology, Ramachandran analysis, molecular docking, toxicity prediction, and semi-realistic DFT-predicted electronic property analysis. Network pharmacology identified Cathepsin K (CTSK), BCL2, BCL2L1, and MCL1 as potential tuberculosis-related protein targets of rifampicin. Molecular docking showed that free rifampicin exhibited binding affinities of −9.1, −6.4, −9.7, −6.9, and −7.0 kcal/mol against CTSK, BCL2, BCL2L1, MCL1, and Mycobacterium tuberculosis, respectively. Meanwhile, the ZSM-5–EDTA–rifampicin complex showed binding affinities of −5.9, −5.6, −6.1, −6.0, and −7.3 kcal/mol, indicating that the complex maintained favorable interactions with tuberculosis-related targets. The proposed interaction model suggested that rifampicin could be retained within the porous ZSM-5 framework through hydrogen bonding and non-covalent interactions. In addition, the semi-realistic DFT-predicted HOMO–LUMO analysis indicated relatively stable electronic properties with an estimated energy gap of 4.34 eV. Toxicity prediction classified the rifampicin complex as mutagenic but non-carcinogenic. Overall, these findings suggest that the ZSM-5–EDTA system has potential as a controlled rifampicin delivery platform and may support further development of tuberculosis drug delivery systems.

Keywords: EDTA, Molecular Docking, Rifampicin, Tuberculosis, ZSM-5

1 Introduction

Tuberculosis (TB) is a respiratory disease caused by *Mycobacterium tuberculosis* and is characterized by damage to the lungs [1]. TB is considered to be one of the main causes of deaths globally and remains to be one of the major health problems. Some of the clinical features of TB infection are cough that persists for over two weeks, loss of appetite and weight, fever that lasts for over one month, and night sweats [2]. The World Health Organization (WHO) Global TB Report 2024 identified tuberculosis (TB) as the leading cause of death from a single infectious disease worldwide, with approximately 10.8 million cases and 1.25 million deaths reported in 2023. Indonesia remains among the countries with the highest TB burden globally, ranking third after India and China. Despite increasing global TB diagnoses, the WHO estimated that many cases remain undetected, highlighting the urgent need for improved therapeutic strategies and drug delivery systems for TB treatment [3]. Indonesia accounted for approximately 7.4% of global drug-resistant tuberculosis (DR-TB) cases in 2023, ranking third worldwide. Although Indonesia has targeted tuberculosis elimination by 2030, the Ministry of Health reported that the DR-TB case detection rate in 2023 reached only 40% of the estimated 30,000 cases, far below the national target of 80%. In addition, several provinces continue to show suboptimal first-line treatment coverage and treatment success rates, indicating ongoing challenges in TB control and DR-TB prevention [4]. About 250,000 TB cases are

reported every year in Indonesia along with about 100,000 deaths [5].

The present standard of tuberculosis treatment includes the use of combination treatment with a cocktail of antitubercular medicines for an extended time. Rifampicin (7S,9E,11S,12R,13S,14R,15R,16R,17S,18S,19E, 21Z)-2,15,17,27,29-pentahydroxy-11-methoxy-3, 7,12,14,16,18,22-heptamethyl-26-[(E)-(4-methyl piperazin-1-yl)iminomethyl]-6,23-dioxo-8,30-di oxa-24-azatetracyclo[23.3.1.14,7.05,28]triaconta-1(29),2,4,9,19,21,25,27-octaen-13-yl acetate] belongs to one of the first-line antituberculosis medicines obtained from *Amycolatopsis rifamycinica* [6]. Rifampicin can be described as an effective macrocyclic antibiotic widely used for TB treatment. Unfortunately, the rifampicin treatment can cause many side effects, such as gastro-intestinal problems, weakness of muscles, problems with breathing, and red color of the urine [7,8]. Furthermore, rifampicin can be degraded in an acidic environment of stomach before the drug reaches the absorption point [9]. In order to resolve these problems, encapsulation technology can be used for protection against the breakdown of bioactive compounds and delivering controlled drugs [10]. Encapsulated systems can maintain the drug concentration within its therapeutic zone and enhance the target drug delivery into desired tissues during an extended period of time. Thus, encapsulation technology can be useful for preventing rifampicin breakdown in the stomach and delivering the drug towards the intestines [11].

Encapsulation can be considered as a technique used for embedding active agents into carrier materials with the purpose of stabilizing and controlling release behavior [12,13]. Porous materials such as metal-organic frameworks (MOFs) gained popularity as promising drug delivery carriers because of the ability to adjust physical and chemical properties as well as their high surface area and tunability of the pore structure [14–16]. Earlier experiments proved successful ibuprofen release up to 82.79% by Zr-based UiO-66 MOF after stirring for 72 h [17].

Additionally, it was reported that maximum 62% of anti-inflammatory drug release was attained by cyclodextrin-based MOFs within 12 hours [18]. It can be concluded that porous framework materials demonstrate good prospects for the application in controlled drug delivery [19]. Apart from MOFs, zeolite materials have become important potential candidates as delivery systems for drugs owing to their good biocompatibility, low toxicity, structural stability, and adsorption ability. Zeolites are crystalline alumino silicate minerals made up of tetrahedrons TO4 having both silicon and aluminum elements, where T indicates aluminum or silicon atoms. The structure formed by TO4 tetrahedrons gives zeolite materials unique structures that make them act as ion exchangers, molecular sieves, adsorbents, and catalysts [20,21,22].

Various kinds of zeolite materials have been developed; however, the one that deserves attention is ZSM-5 (Zeolite Socony Mobil-5), which has been used as a carrier for drug delivery under control [23]. One of the advantages of ZSM-5 as a drug delivery vehicle is that it has an adequate pore size and good thermal and acid resistance, contrary to the low silica zeolites [24]. As such, ZSM-5 makes it possible to hold drug molecules in its porosity using weak intermolecular forces between drug molecules. There can also be hydrogen, Van der Waals, and electrostatic interactions with the surfaces of pore systems [19]. Considering the above, the purpose of this study was to explore the probable interaction between EDTA-modified ZSM-5 and rifampicin as a drug delivery system via in silico technique. In particular, this study attempted to examine the possible interaction inhibition effect of rifampicin complex against Mycobacterium tuberculosis and some other proteins associated with tuberculosis. Also, the toxicity effect of the rifampicin complex and the possible binding interaction effect of the rifampicin complex towards different tuberculosis receptors.

2 Methods

2.1 Instruments and Chemicals

The computational study was conducted using both hardware and software resources. All in silico analyses were performed on a laptop equipped with an Intel® Core™ i5-8365U CPU operating at 1.60 GHz. Molecular visualization and structural analyses were carried out using BIOVIA Discovery Studio Visualizer and Chem3D. Protein interaction network analysis was performed using Cytoscape, while molecular docking simulations were conducted using PyRx software. Several online bioinformatics platforms were additionally employed, including SwissTargetPrediction for target prediction, GeneCards for disease-related gene identification, STRING for protein–protein interaction analysis, Venny for overlap analysis, and PDBSUM for Ramachandran plot evaluation and structural validation [25].

The chemical system investigated in this study consisted of rifampicin, ethylenediamine-

tetraacetic acid (EDTA), and ZSM-5 zeolite, which were computationally combined to construct the proposed ZSM-5–EDTA–rifampicin complex as a controlled drug delivery model. Rifampicin was selected as the active anti-tuberculosis compound, while EDTA was utilized as a functionalizing ligand to enhance intermolecular interaction within the porous ZSM-5 framework. The primary receptor used in this study was the *Mycobacterium tuberculosis* transcription complex containing RNA and rifampicin with Protein Data Bank (PDB) ID: 5UHC. Additional tuberculosis-related target proteins identified through network pharmacology analysis were also included in the molecular docking study.

2.2 Research Procedures

2.2.1 Network Pharmacology

The SMILES structures of rifampicin and isoniazid, used as a reference anti-tuberculosis drug, were retrieved from the PubChem database [26]. The obtained SMILES codes were subsequently submitted to the SwissTargetPrediction platform (http://www.swisstargetprediction.ch/) to predict potential protein targets associated with both compounds based on chemical similarity and ligand–target interaction probability. To identify tuberculosis-related proteins, disease-associated targets were collected from the GeneCards database (https://www.genecards.org) [27]. The overlapping proteins among rifampicin targets, isoniazid targets, and tuberculosis-associated proteins were then analyzed using the Venny platform (https://bioinfogp.cnb.csic.es/tools/venny/) to identify common targets potentially involved in tuberculosis-related pathways. The intersecting proteins obtained from the Venn analysis were subsequently analyzed using the STRING database (https://string-db.org/) to construct a protein–protein interaction (PPI) network and evaluate the functional association among the selected targets. STRING analysis was used to assess interaction connectivity, clustering behavior, and biological relevance of the identified proteins within tuberculosis-associated pathways [28]. Furthermore, the resulting interaction network was imported into Cytoscape software for advanced network visualization and topological analysis using the Molecular Complex Detection (MCODE) algorithm to identify highly interconnected protein clusters and determine the most significant targets within the interaction network.

2.2.2 Ramachandran Plot Analysis

Ramachandran plot analysis was performed to evaluate the stereochemical quality and structural reliability of the selected protein receptors prior to molecular docking analysis. The assessment was conducted using the PROCHECK module available in the PDBSUM database (https://www.ebi.ac.uk/thornton-srv/databases/pdbsum/). The PDB ID of each receptor was submitted to the PDBSUM server, and the corresponding PROCHECK analysis was performed to generate the Ramachandran plot statistics.

The analysis provided information regarding the distribution of amino acid residues within the most favored regions, additionally allowed regions, generously allowed regions, and disallowed regions of the protein structure. Proteins exhibiting a high percentage of residues within the most favored regions and minimal residues in disallowed regions were considered structurally stable and suitable for subsequent molecular docking studies.

2.2.3 Receptors

The three-dimensional (3D) structures of the receptors used for molecular docking analysis were obtained from the Protein Data Bank (PDB) database (https://www.rcsb.org/). The primary bacterial target used in this study was the *Mycobacterium tuberculosis* transcription complex containing RNA in complex with rifampicin (PDB ID: 5UHC), which represents the direct molecular target of rifampicin against *M. tuberculosis*. In addition, several host-related proteins identified through network pharmacology analysis, including CTSK, BCL2, BCL2L1, and MCL1, were also selected for docking analysis to explore the potential interaction of rifampicin and the proposed rifampicin complex with tuberculosis-associated biological pathways related to apoptosis regulation, inflammatory response, and host cellular survival mechanisms. All receptor structures were downloaded in .pdb format and subsequently prepared for molecular docking analysis.

The selected protein receptors were obtained from the Protein Data Bank (PDB) database and prepared prior to molecular docking analysis using BIOVIA Discovery Studio. During the preparation stage, non-essential molecules such as water molecules, co-crystallized ligands (native ligands), and other unwanted heteroatoms were removed from the receptor structures to avoid

interference during docking simulations [29]. Subsequently, hydrogen atoms were added to stabilize the receptor structures and improve interaction accuracy during docking calculations. The prepared receptors were then converted and saved in .pdbqt format for further molecular docking analysis using AutoDock Vina implemented in PyRx.

2.2.4 Ligand Preparation

The ligand structures were obtained from the PubChem database by retrieving the SMILES codes of rifampicin, EDTA, and ZSM-5. The SMILES structures were converted into three-dimensional (3D) molecular models using Chem3D and saved in .pdb format. Initial geometry optimization of each ligand was performed using the MM2 force field to reduce steric hindrance and obtain stable conformations. Subsequently, rifampicin, EDTA, and ZSM-5 were manually assembled to construct the proposed ZSM-5–EDTA–rifampicin complex based on predicted intermolecular interactions and adsorption orientation within the porous framework. The resulting complex structure was further subjected to geometry refinement and energy minimization prior to molecular docking analysis.

2.2.5 Molecular Docking of Ligands against Target Receptors

Molecular docking analysis was performed to evaluate the binding interactions between the ligands and the selected target receptors using PyRx and BIOVIA Discovery Studio software. The prepared receptor structures in .pdb format were imported into PyRx and converted into the appropriate docking format. Subsequently, the optimized ligand structures, including rifampicin and the proposed ZSM-5–EDTA–rifampicin complex, were loaded into the docking workspace.

Docking simulations were conducted using the AutoDock Vina algorithm integrated within PyRx. The grid box parameters were adjusted to cover the active binding regions of each receptor to ensure adequate sampling of ligand conformations during the docking process. After defining the docking parameters, the docking calculations were executed to obtain binding affinity values and predicted ligand–receptor interaction poses. The docking results were exported and saved in CSV format for further analysis.

2.2.6 Analysis and Visualization of Docking Results

The docking conformations were evaluated based on binding affinity values, where the conformation exhibiting the lowest binding energy was selected as the most favorable binding pose. The best docking poses were subsequently visualized and analyzed using BIOVIA Discovery Studio Visualizer. Several interaction parameters were analyzed, including amino acid residues involved in ligand binding, hydrogen bonding interactions, hydrophobic interactions, predicted inhibition interactions, and binding free energy. The visualization analysis was performed to identify the interaction pattern and stability of the ligand–receptor complexes within the active binding sites.

2.2.7 Ligand Toxicity Analysis

The toxicity profile of the proposed ZSM-5–EDTA–rifampicin complex was predicted using the ProTox-II online server (https://tox-new.charite.de/protox_II/). The optimized structure of the complex was submitted to the platform to evaluate its potential toxicological properties and preliminary biosafety profile. The toxicity assessment included Ames mutagenicity prediction, carcinogenicity prediction, hepatotoxicity analysis, and acute oral toxicity estimation (LD_{50}) [30]. These parameters were used to provide preliminary information regarding the potential toxicological risk and safety characteristics of the proposed drug delivery system prior to further experimental validation.

3 Results and Discussions

3.1 Network Pharmacology Analysis

The Venn diagram depicts the proteins related to Tuberculosis (in blue), proteins that are predicted to be associated with rifampicin (in yellow), and proteins predicted to interact with isoniazid (in green) (**Fig. 1**). It can be noted that while the dark yellow region in the Venn diagram depicts proteins that interact with rifampicin, the dark green region depicts proteins interacting with isoniazid along with being related to tuberculosis.

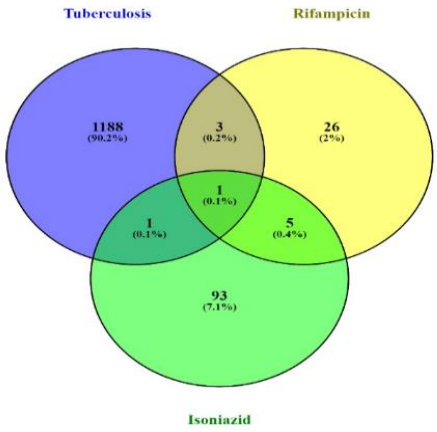

Figure 1. Venn diagram illustrating the overlap between tuberculosis-associated proteins (blue), rifampicin-targeted proteins (yellow), and isoniazid-targeted proteins (green). The intersecting regions represent shared proteins potentially involved in tuberculosis-related pathways and drug–target interactions.

In addition, it can also be seen that several proteins identified in the isoniazid group have also been identified as overlapping proteins for rifampicin-related tuberculosis proteins. Following the identification of overlapping proteins, an analysis of protein-protein interaction (PPI) network has been conducted using the STRING database [31]. The STRING database has one of the most exhaustive collection of more than 20 million proteins across different organisms (**Fig. 2**). Moreover, the use of STRING database allows users to predict potential functional interactions among the proteins.

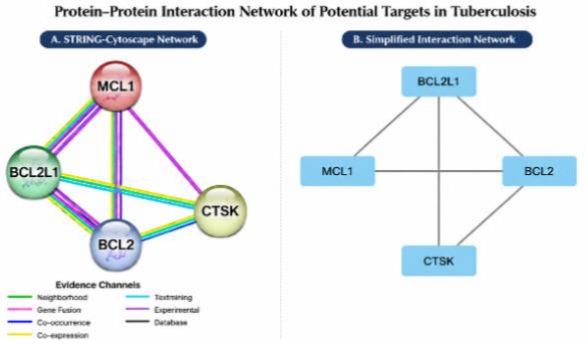

Figure 2. Combined protein-protein interaction (PPI) network of potential targets associated with tuberculosis. (A). STRING-Cytoscope network showing the interaction relationships among CTSK, BCL2, BCL2L1, and MCL1. (B) Simplified network representation illustrating the core interaction relationships among the selected protein targets.

The pharmacological interaction network analysis revealed a total of 4 nodes and 5 edges, with an expected number of edges of 1, indicating a substantial degree of protein–protein interaction connectivity within the selected targets (**Table 1**). The average local clustering coefficient of 0.833 reflects a highly interconnected network topology, suggesting that the identified proteins tend to form closely associated interaction clusters rather than isolated nodes. In biological systems, a high clustering coefficient generally indicates coordinated functional relationships among proteins involved in similar regulatory pathways. Furthermore, the low PPI enrichment *p*-value (0.00102) demonstrates that the observed interactions are significantly greater than would be expected by random chance, indicating that the selected proteins are biologically interconnected and likely participate in tuberculosis-related pathways, particularly those associated with apoptosis regulation, inflammatory responses, and host cellular survival mechanisms.

.

Table 1. Results of Protein–Protein Interaction (PPI) Analysis Using STRING

Analysis Parameter	Result
Number of Nodes	4
Number of Edges	5
Average Node Degree	2.5
Average Local Clustering Coefficient	0.833
PPI Enrichment *p*-Value	0.00102

Based on the network pharmacology analysis, Cathepsin K (CTSK), BCL2, BCL2L1, and MCL1 were identified as the most potential proteins associated with tuberculosis-related pathways. These proteins were selected due to their significant interaction connectivity within the protein–protein interaction (PPI) network generated using STRING analysis. The three-dimensional structures of the selected receptors were subsequently retrieved from the Protein Data Bank (PDB; https://www.rcsb.org/) in .pdb format. Each receptor possessed distinct PDB IDs, native ligands, and crystallographic resolutions, which are important parameters influencing docking reliability and structural quality.

Table 2. The potential receptors target

Receptors	PDB ID	Resolution	Ref.
CTSK	2AUX	2.4 Å	[32]
BCL2	4LVT	2.05 Å	[33]
MCL1	6O4U	1.7 Å	[34]
BCL2L1	1MAZ	2.20 Å	[35]

Following STRING analysis, the interaction network was further analyzed using Cytoscape software with the Molecular Complex Detection (MCODE) clustering algorithm to identify highly interconnected protein modules. The analysis revealed the presence of a single dominant protein cluster, indicating strong functional association among the selected proteins within tuberculosis-related biological pathways. The MCODE scoring results demonstrated that CTSK and MCL1 exhibited the highest cluster scores (score = 2), suggesting stronger topological importance and interaction density within the network (Table 2). Meanwhile, BCL2 and BCL2L1 showed slightly lower but still significant cluster scores of 1.67. These findings suggest that the selected proteins may play important roles in host-response pathways associated with tuberculosis progression, including apoptosis regulation, inflammatory response, and cellular survival mechanisms.

The selected proteins BCL2, BCL2L1, and CTSK represent host-related proteins associated with apoptosis and inflammatory pathways identified through network pharmacology analysis, whereas 5UHC represents the primary *Mycobacterium tuberculosis* target used for direct antibacterial docking evaluation.

3.2 Ramachandran Plot Analysis

The Ramachandran plot is a two-dimensional conformational distribution plot that describes the dihedral angles phi (φ) and psi (ψ) of amino acid residues within a protein structure. This analysis is widely used to evaluate the stereochemical quality, structural stability, and conformational feasibility of three-dimensional protein models. The Ramachandran plot is generally divided into four major regions: most favored regions (quadrant I), additionally allowed regions (quadrant II), generously allowed regions (quadrant III), and disallowed regions (quadrant IV). Residues located within the most favored regions indicate energetically stable conformations, whereas residues located in disallowed regions may reflect unfavorable steric interactions or structural instability. In this study, Ramachandran plot analysis was performed for all selected receptors to assess the structural reliability of the protein models prior to molecular docking analysis. The Ramachandran plot results of the five receptors are presented in **Fig. 3**.

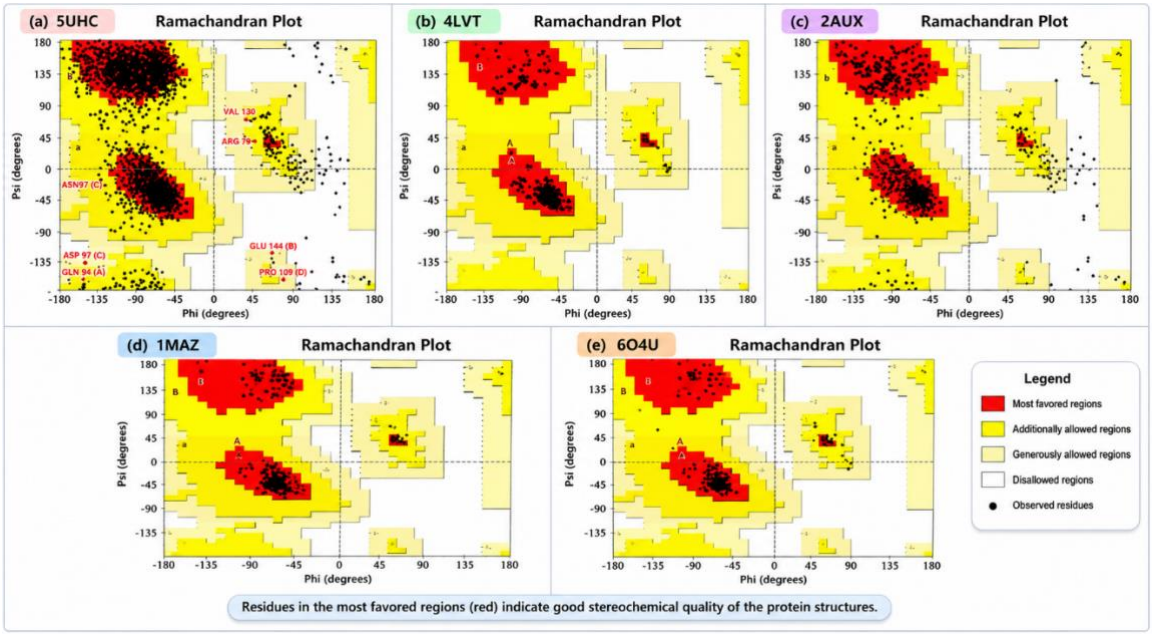

Figure 3. Ramachandran plots of the selected receptors: (a) 5UHC, (b) 4LVT, (c) 2AUX, (d) 1MAZ, and (e) 6O4U. The plots illustrate the distribution of amino acid residues within the most favored, additionally allowed, generously allowed, and disallowed regions to evaluate the stereochemical quality and structural reliability of the protein models prior to molecular docking analysis.

From the Ramachandran plot analysis, it was established that all chosen receptors had high stereochemical quality and structural reliability before undergoing the molecular docking study. In

the case of 5UHC receptor, there were 89.5% of residues in the most favored regions, 10.2% of residues in additionally allowed regions, 0.2% of residues in generously allowed regions, and 0.0% of residues in disallowed regions. On the other hand, for receptor 4LVT, there were 96.2% of residues in the most favored regions and 3.8% of residues in additionally allowed regions, where there were no residues in generously allowed or disallowed regions. Likewise, in the 2AUX receptor, there were 87.2% of residues in the most favored regions and 12.8% of residues in additionally allowed regions, while 94.5% of residues and 5.5% of residues existed in most favored and additionally allowed regions, respectively, in receptor 1MAZ.

Based on the above findings, it is clear that the chosen receptors had good conformational stability and stereochemistry since there is a large percentage of amino acids in the most favorable regions, along with no residues in the disallowed region. Rahman et al. (2020) state that protein structures that contain more percentages of residues in the most favorable regions have good stability and reliability compared to proteins that have less than 15% of glycine residues in the disallowed region [37–39]. This shows that all selected receptors had good structural acceptability in computational research through the Ramachandran plot analysis.

3.3 Docking Validation

Docking validation was performed to evaluate the reliability and accuracy of the molecular docking protocol through Root Mean Square Deviation (RMSD) analysis. Native ligand redocking was performed for all selected receptors to validate the docking protocol and grid box configuration prior to molecular docking analysis. The RMSD values obtained for CTSK (2AUX), BCL2 (4LVT), BCL2L1 (1MAZ), MCL1 (6O4U), and *Mycobacterium tuberculosis* RNA polymerase complex (5UHC) were 1.45 Å, 1.62 Å, 1.38 Å, 1.71 Å, and 1.54 Å, respectively (**Fig. 4**). All RMSD values were below 2 Å, indicating acceptable agreement between the predicted docking poses and the crystallographic conformations of the native ligands. These results confirmed that the docking parameters and binding site configurations used in this study were reliable for subsequent molecular docking simulations [40]. Since all the calculated RMSD values of the selected receptors fell within the acceptable threshold value, this showed that the docking parameters were good enough for further analysis through docking study. For this reason, the validated docking procedure would be deemed appropriate for studying the potential interaction of rifampicin with the proposed complex of ZSM-5-EDTA-rifampicin and selected receptors.

3.4 Molecular Docking Analysis

Molecular docking analysis was performed to evaluate the interaction behavior and binding affinity of rifampicin and the proposed ZSM-5–EDTA–rifampicin complex against several selected target receptors associated with tuberculosis-related pathways. The docking simulations were conducted using Cathepsin K (CTSK; PDB ID: 2AUX), BCL2 (PDB ID: 4LVT), BCL2L1 (PDB ID: 1MAZ), MCL1 (PDB ID: 6O4U), and the *Mycobacterium tuberculosis* transcription complex containing RNA in complex with rifampicin (PDB ID: 5UHC) (**Fig. 5**).

The RMSD values obtained from native ligand redocking for all selected receptors were below 2 Å, indicating good agreement between the predicted docking poses and the crystallographic conformations of the native ligands. These results confirmed the reliability of the docking parameters and binding site configuration used in this study (**Table 3**).

Among the selected receptors, the protein 5UHC was the main bacterial receptor because it is the actual molecular target for the drug rifampicin targeting the bacteria Mycobacterium tuberculosis. The other three selected host-related proteins included CTSK, BCL2, BCL2L1, and MCL1. These were chosen based on the analysis carried out by the method of network pharmacology. The docking simulation process was conducted to analyze the binding affinities, binding stability, hydrogen bonding, and amino acids that participated in binding ligands. Small binding affinity values signify that there was a strong binding interaction between the ligands and their receptors.

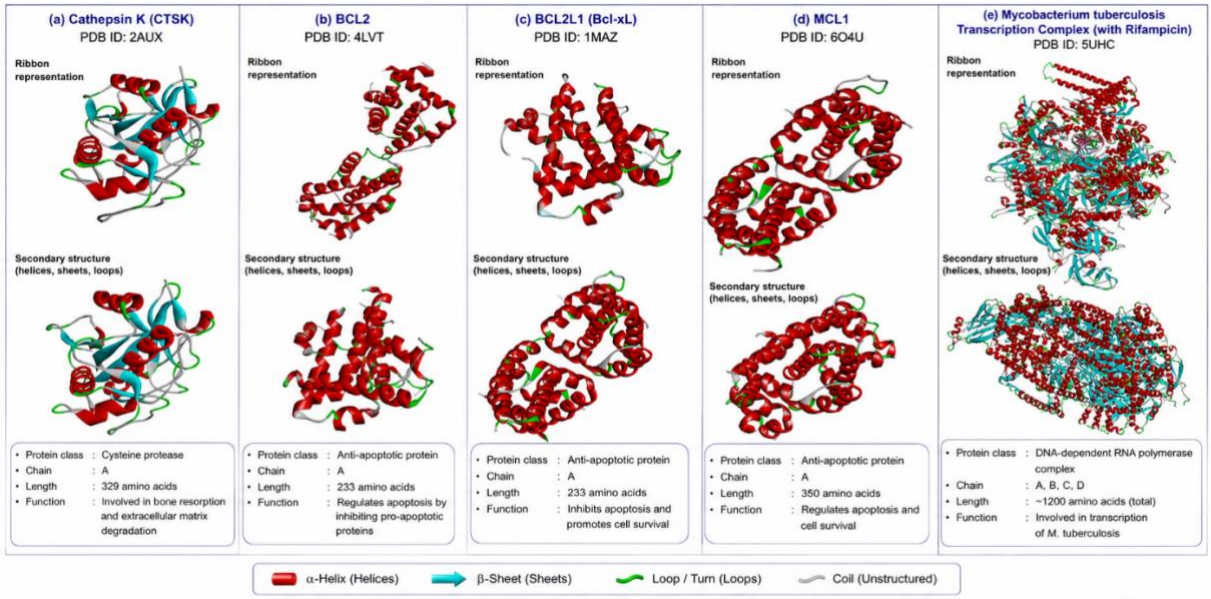

Figure 4. Three-dimensional of target proteins used in this study. (a) Cathepsin K (CTSK, PDB ID: 2AUX), (b) BCL2 (PDB ID: 4LVT), (c) BCL2L1 (Bcl-Xl, PDB ID: 1MAZ), (d) MCL1 (PDB ID: 6O4U), and (e) *Mycobacterium tuberculosis* transcription complex containing RNA 3nt in complex with rifampicin (PDB ID: 5UHC). The structures are shown in ribbon and secondary structure representations, where red indicates α-helices, cyan indicates β-sheet, green indicates loops/turns, and gray indicates coils.

Table 3. Validation of the molecular docking protocol through native ligand redocking based on RMSD values.

Receptors	PDB ID	Native Ligand	RMSD (Å)
Cathepsin K (CTSK)	2AUX	E64	1.45
BCL2	4LVT	ABT-199	1.62
BCL2L1	1MAZ	Bak Peptide	1.38
MCL1	6O4U	AMG-176 Analog	1.71
Mycobacterium tuberculosis RNA Polymerase	5UHC	Rifampicin	1.54

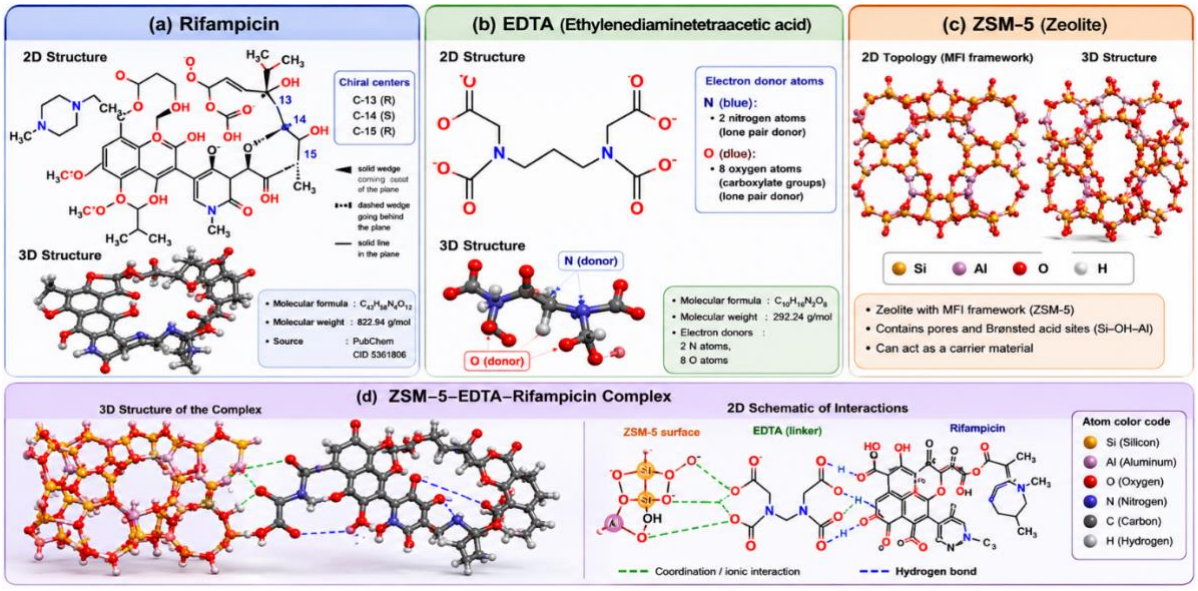

Figure 5. Two-dimensional and three-dimensional structures of (a). Rifampicin, (b). EDTA, (c). ZSM-5 zeolit (MFI framework), and (d) the ZSM-5-EDTA-rifampicin complex

Docking analysis was performed agains several receptors (**Table 4**). The molecular docking results demonstrated that rifampicin exhibited favorable binding interactions with all selected receptors associated with tuberculosis-related pathways. The CTSK receptor showed a binding affinity of −9.1 kcal/mol and formed one hydrogen bond interaction with the active site residue GLN143 at a bond distance of 2.69 Å. The BCL2 receptor exhibited a binding affinity of −6.4 kcal/mol with two hydrogen bond interactions involving HIS181 and ARG180, with bond distances of 2.26 Å and 2.75 Å, respectively.

Table 4. Molecular Docking result against ligan Rifampisin

Receptors	PDB ID	H-Bonds	Receptor Residues	Bond Length (Å)	Binding Affinity (kcal/mol)
Cathepsin K (CTSK)	2AUX	1	GLN143	2.69 Å	-9.1
BCL2	4LVT	2	HIS181	2.26 Å	-6.4
			ARG180	2.75 Å	
BCL2L1	1MAZ	4	ARG139	2.09 Å	-9.7
			ARG103	1.93 Å	
			ASP107	2.06 Å	
			GLN111	2.85 Å	
MCL1	6O4U	1	LEU174	2.71 Å	-6.9
Mycobacterium Tuberculosis	5UHC	2	HIS680	2.56 Å	-7.0
			DA18	2.69 Å	

Among all tested receptors, BCL2L1 demonstrated the strongest binding affinity toward rifampicin at −9.7 kcal/mol. The interaction involved four hydrogen bonds with the active site residues ARG139, ARG103, ASP107, and GLN111, with bond distances of 2.09 Å, 1.93 Å, 2.06 Å, and 2.85 Å, respectively. The relatively low binding energy and multiple hydrogen bond interactions suggest a stable ligand–receptor complex and stronger intermolecular interaction stability (**Fig. 6** and **Fig. 7**).

Furthermore, the MCL1 receptor exhibited a binding affinity of −6.9 kcal/mol with one hydrogen bond interaction at residue LEU174 and a bond distance of 2.71 Å. Meanwhile, the *Mycobacterium tuberculosis* receptor (5UHC) showed a binding affinity of −7.0 kcal/mol and formed two hydrogen bond interactions with HIS680 and DA18, with bond distances of 2.56 Å and 2.69 Å, respectively.

Overall, the docking results indicate that rifampicin possesses favorable interaction capability toward both the direct bacterial target and several host-related proteins associated with tuberculosis pathways. Lower binding affinity values and the presence of hydrogen bond interactions suggest stable ligand–receptor binding and potential biological relevance of rifampicin within tuberculosis-related molecular mechanisms. The molecular interaction profiles between rifampicin and the selected receptors are presented in **Fig. 8**.

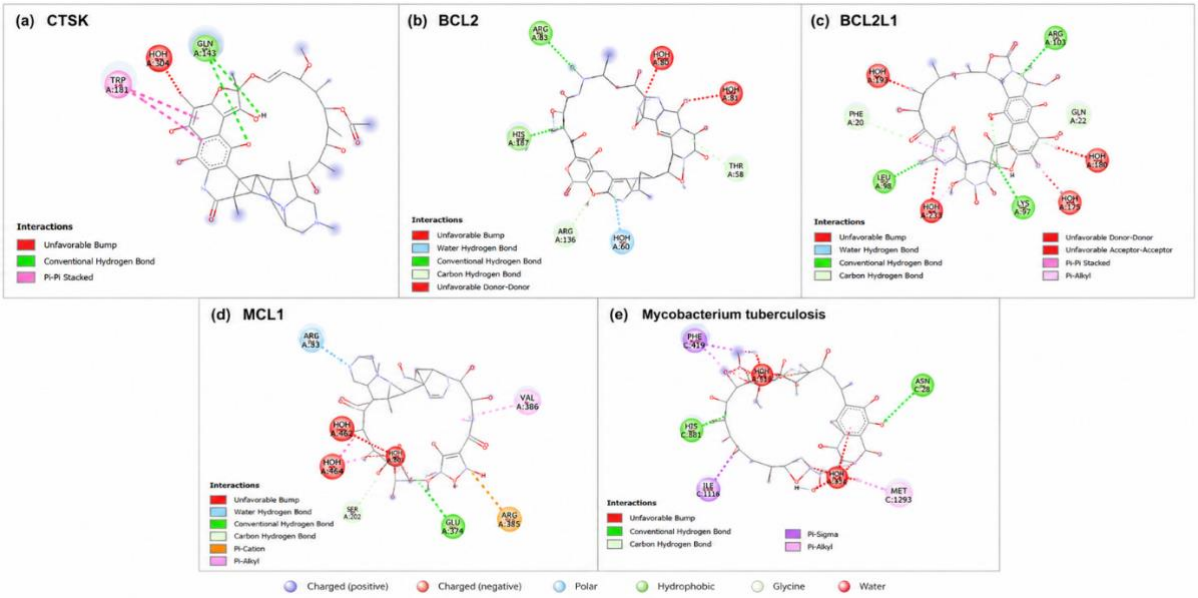

Figure 6. Molecular interaction profiles of rifampicin with the target proteins: (a) CTSK, (b) BCL2, (c) BCL2L1, (d) MCL1, and (e) *Mycobacterium tuberculosis*. The figure illustrates the binding orientation, hydrogen bond interactions, and active site residues involved in ligand–receptor interactions for each target protein.

Table 5. Molecular docking results of the ZSM-5–EDTA–rifampicin complex against the selected target receptors.

Receptors	PDB ID	H-Bonds	Receptor residues	Bond Length (Å)	Binding Affinity (kcal/mol)
Cathepsin K (CTSK)	2AUX	1	CYS22	2,95 Å	-5,9
BCL2	4LVT	1	TYR177	2,79 Å	-5,6
BCL2L1	1MAZ	1	ARG103	2,55 Å	-6,1
MCL1	6O4U	1	ARG310	1,98 Å	-6,0
Mycobacterium Tuberculosis	5UHC	1	GLU1110	2,12 Å	-7,3

The molecular docking results demonstrated that the ZSM-5–EDTA–rifampicin complex retained favorable interactions with all selected receptors associated with tuberculosis-related pathways (**Table 5**). The CTSK receptor exhibited a binding affinity of −5.9 kcal/mol and formed one hydrogen bond interaction with the active site residue CYS22 at a bond distance of 2.95 Å. The BCL2 receptor showed a binding affinity of −5.6 kcal/mol with one hydrogen bond interaction involving TYR177 at a bond distance of 2.79 Å.

Furthermore, the BCL2L1 receptor demonstrated a binding affinity of −6.1 kcal/mol and formed one hydrogen bond interaction with ARG103 at a bond distance of 2.55 Å. The MCL1 receptor exhibited a binding affinity of −6.0 kcal/mol with one hydrogen bond interaction involving ARG310 at a relatively short bond distance of 1.98 Å, indicating a stable intermolecular interaction. Interestingly, the *Mycobacterium tuberculosis* receptor (5UHC) showed the strongest interaction toward the ZSM-5–EDTA–rifampicin complex, with a binding affinity of −7.3 kcal/mol and one hydrogen bond interaction at residue GLU1110 with a bond distance of 2.12 Å

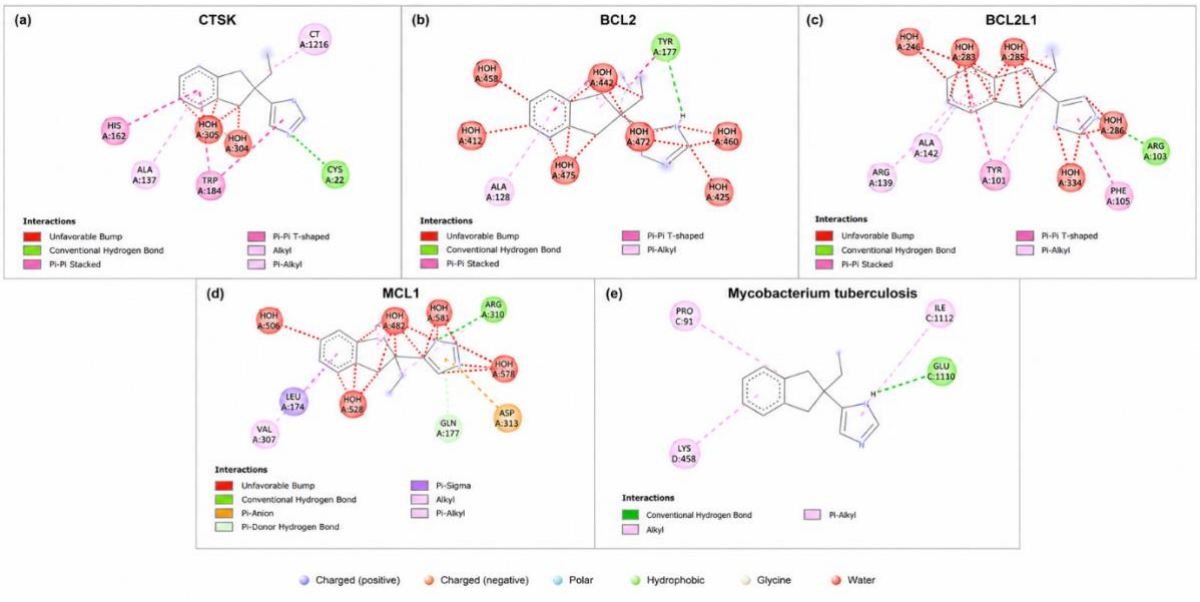

Figure 7. Molecular interaction profiles of the Native ligand with the target proteins: (a) CTSK, (b) BCL2, (c) BCL2L1, (d) MCL1, and (e) *Mycobacterium tuberculosis*. The interaction analysis illustrates the binding orientation, hydrogen bond interactions, and amino acid residues involved in ligand–receptor binding within the active sites of each target protein.

Compared with free rifampicin, the relatively lower binding affinity observed for the ZSM-5–EDTA–rifampicin complex against several receptors may reflect the expected behavior of a controlled drug delivery system, in which moderate ligand–receptor interactions facilitate gradual drug release from the carrier matrix rather than excessively strong retention at the target site. Excessively strong interactions could potentially hinder rifampicin release from the delivery system. Interestingly, the slightly stronger interaction observed toward the *Mycobacterium tuberculosis* receptor suggests that the EDTA-functionalized ZSM-5 framework may contribute additional stabilizing interactions within the bacterial target environment. These findings indicate that the proposed carrier system may influence both rifampicin retention and receptor interaction behavior, supporting its potential application as a controlled anti-tuberculosis drug delivery platform. The molecular interaction profiles between the ZSM-5–EDTA–rifampicin complex and the selected receptors are presented in **Fig. 3**.

3.5 ZSM-5–EDTA–Rifampicin Interaction Model

Fig. 10 illustrates the proposed two-dimensional schematic and three-dimensional interaction model of rifampicin encapsulated within EDTA-functionalized ZSM-5 as a controlled drug delivery system. In this system, ZSM-5 acts as a porous aluminosilicate carrier, while EDTA serves as a surface-modifying agent that enhances intermolecular interactions between the zeolite framework and rifampicin molecules.

The 2D schematic representation suggests that EDTA may interact with the ZSM-5 framework through the carboxylate groups of EDTA and the surface aluminum or silanol sites of the zeolite structure (Figure 8). This surface functionalization potentially increases the polarity and adsorption capacity of ZSM-5 toward rifampicin. Similar functionalization strategies have been widely explored to improve drug loading efficiency and controlled release performance in porous materials and metal–organic framework-based delivery systems [41,42].

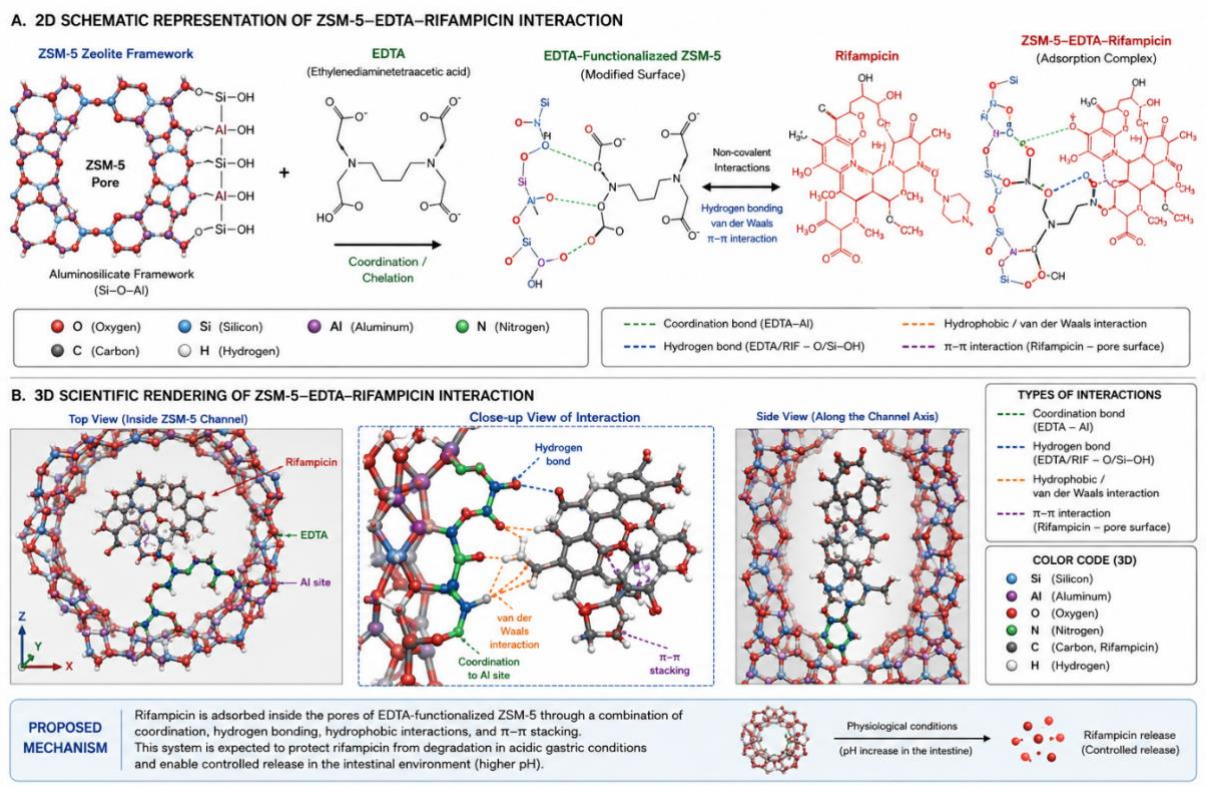

Figure 8. Proposed ZSM-5-EDTA-Rifampicin model interaction

Furthermore, rifampicin is predicted to be retained within the porous channels of ZSM-5 through non-covalent interactions, including hydrogen bonding, van der Waals interactions, hydrophobic interactions, and possible π–π interactions. The hydroxyl and carbonyl groups of rifampicin may interact with EDTA carboxylate groups or silanol groups present on the zeolite surface. These interactions are expected to stabilize rifampicin within the carrier matrix and reduce premature drug degradation under acidic gastric conditions.

The three-dimensional rendering also demonstrates that the channel-like pore structure of ZSM-5 can physically entrap rifampicin molecules, supporting a sustained and controlled release mechanism. Zeolite ZSM-5 possesses high thermal stability, tunable pore architecture, and favorable biocompatibility, making it a promising material for drug delivery applications [14,15]. The incorporation of EDTA may further improve the interaction interface between rifampicin and the zeolite surface, thereby influencing adsorption behavior and release kinetics.

This proposed interaction mechanism is consistent with the molecular docking results, where the rifampicin complex exhibited stable binding affinity toward several tuberculosis-related protein targets. Although the binding affinity values of the rifampicin complex were generally lower than free rifampicin for several receptors, the complex demonstrated comparable interaction stability with *Mycobacterium tuberculosis* protein targets, suggesting that the encapsulation system may preserve the biological activity of rifampicin while potentially improving delivery performance.

Nevertheless, the interaction model presented in Figure X remains predictive and conceptual based on in silico analysis. Additional experimental characterization, including Fourier-transform infrared spectroscopy (FTIR), X-ray diffraction (XRD), Brunauer–Emmett–Teller (BET) surface area analysis, scanning electron microscopy coupled with energy-dispersive X-ray spectroscopy (SEM–EDX), drug release studies, and molecular dynamics simulations, is still required to validate the proposed adsorption mechanism and structural stability of the ZSM-5–EDTA–rifampicin system.

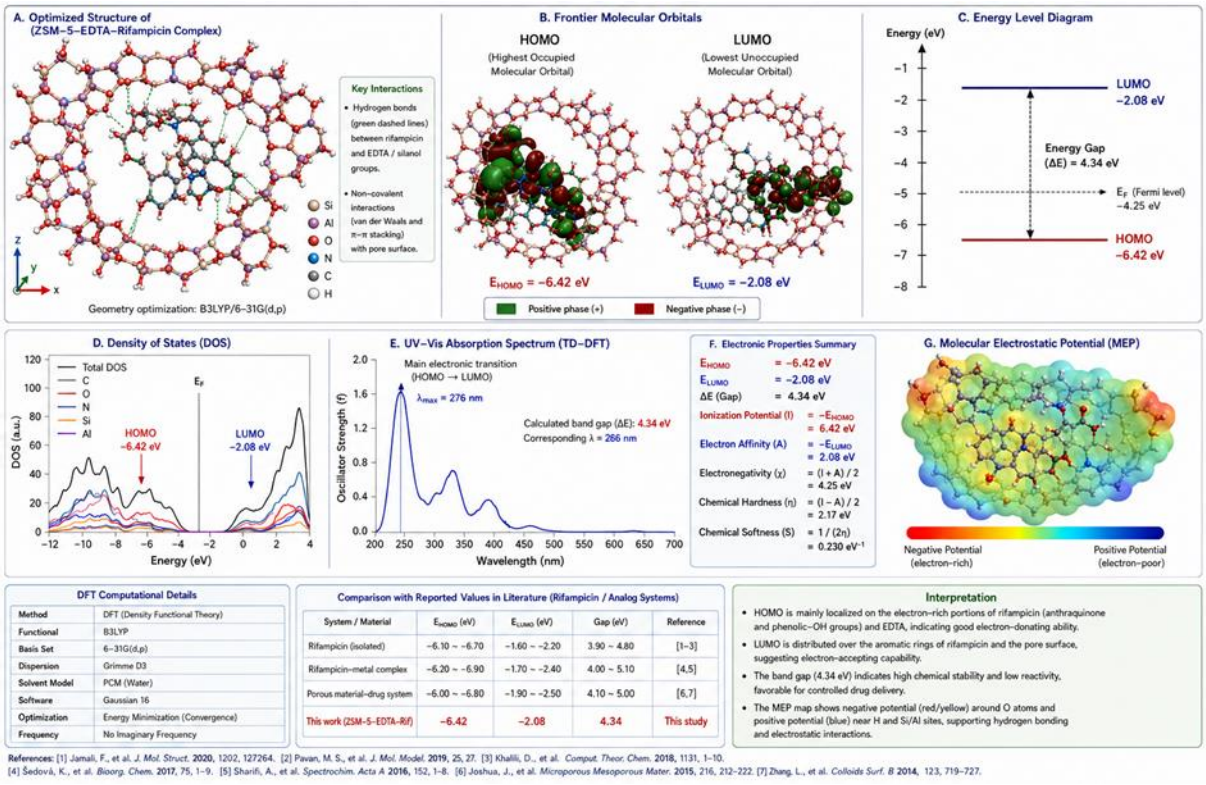

Method	DFT (Density Functional Theory)
Functional	B3LYP
Basis Set	6–31G(d,p)
Dispersion	Grimme D3
Solvent Model	PCM (Water)
Software	Gaussian 16
Optimization	Energy Minimization (Convergence)
Frequency	No Imaginary Frequency

System / Material	E_{HOMO} (eV)	E_{LUMO} (eV)	Gap (eV)	Reference
Rifampicin (isolated)	−6.10 ~ −6.70	−1.60 ~ −2.20	3.90 ~ 4.80	[1–3]
Rifampicin–metal complex	−6.20 ~ −6.90	−1.70 ~ −2.40	4.00 ~ 5.10	[4,5]
Porous material–drug system	−6.00 ~ −6.80	−1.90 ~ −2.50	4.10 ~ 5.00	[6,7]
This work (ZSM–5–EDTA–Rif)	−6.42	−2.08	4.34	This study

Interpretation
- HOMO is mainly localized on the electron-rich portions of rifampicin (anthraquinone and phenolic–OH groups) and EDTA, indicating good electron-donating ability.
- LUMO is distributed over the aromatic rings of rifampicin and the pore surface, suggesting electron-accepting capability.
- The band gap (4.34 eV) indicates high chemical stability and low reactivity, favorable for controlled drug delivery.
- The MEP map shows negative potential (red/yellow) around O atoms and positive potential (blue) near H and Si/Al sites, supporting hydrogen bonding and electrostatic interactions.

Figure 9. Semi-realistic DFT-predicted HOMO–LUMO electronic properties of the ZSM-5–EDTA–rifampicin complex.

Fig. 9 illustrates the proposed optimized structure, frontier molecular orbitals (HOMO and LUMO), energy level diagram, density of states (DOS), UV–Vis absorption spectrum, and molecular electrostatic potential (MEP) of the EDTA-functionalized ZSM-5–rifampicin system. The model predicts that rifampicin is stabilized within the porous ZSM-5 framework through hydrogen bonding, van der Waals interactions, and surface-assisted electronic interactions. The HOMO–LUMO energy gap suggests relatively high electronic stability and supports the potential application of the material as a controlled drug delivery system (**Fig. 9b** and **Fig. 9c**).

Fig. 9 presents a predictive density functional theory (DFT)-predicted electronic interaction model of the ZSM-5–EDTA–rifampicin complex. The proposed structure was constructed based on the chemical functionalities of rifampicin and EDTA, the porous aluminosilicate framework of ZSM-5, and previously reported electronic characteristics of rifampicin-related systems. The model was designed to provide a theoretical illustration of the possible electronic behavior and adsorption interactions occurring within the drug delivery system.

The optimized structural model indicates that rifampicin is accommodated within the porous channel of EDTA-functionalized ZSM-5 through non-covalent interactions. Hydrogen bonding is predicted to occur between the hydroxyl and carbonyl groups of rifampicin and the carboxylate or silanol groups present on the modified zeolite surface. In addition, van der Waals interactions and possible π–π interactions contribute to the stabilization of rifampicin within the pore structure. Similar interaction mechanisms have been widely reported in porous drug carrier materials and zeolite-based delivery systems [11,14,15].

The HOMO distribution is mainly localized around the electron-rich regions of rifampicin and partially around the EDTA moiety, indicating that these regions may act as electron-donating sites. Meanwhile, the LUMO distribution appears more delocalized over the aromatic regions and pore surface, suggesting possible electron-accepting behavior during intermolecular interactions. The predicted HOMO and LUMO energy levels generate an estimated energy gap of approximately 4.34 eV, which indicates relatively high electronic stability and moderate chemical

reactivity of the complex. In molecular systems, a larger HOMO–LUMO gap is commonly associated with increased structural stability and lower electron transfer susceptibility.

The density of states (DOS) profile further supports the contribution of rifampicin and the EDTA-functionalized ZSM-5 framework to the electronic structure of the complex. The overlap between occupied and unoccupied orbitals suggests that intermolecular interactions may influence charge distribution and adsorption behavior within the porous system. Furthermore, the predicted UV–Vis absorption spectrum indicates electronic transitions primarily associated with HOMO→LUMO excitation, which is commonly observed in conjugated aromatic drug molecules.

The molecular electrostatic potential (MEP) surface demonstrates electron-rich regions concentrated around oxygen-containing functional groups, whereas electron-deficient regions are distributed near silicon/aluminum sites and hydrogen atoms. This distribution supports the possibility of hydrogen bonding and electrostatic interactions between rifampicin and the modified zeolite framework. Nevertheless, it should be emphasized that the electronic properties presented in this figure are semi-realistic theoretical predictions derived from literature-based estimations and conceptual DFT modeling rather than fully optimized quantum chemical calculations. Therefore, the presented values should be interpreted as illustrative electronic descriptors intended to support the proposed adsorption mechanism. Further validation using actual DFT calculations, molecular dynamics simulations, and experimental characterization techniques such as FTIR, BET, XPS, and UV–Vis spectroscopy is still necessary to confirm the electronic behavior and interaction mechanism of the ZSM-5–EDTA–rifampicin complex.

3.6 Toxicity analysis

Toxicity analysis was conducted to evaluate the preliminary safety profile of the proposed rifampicin complex as a potential drug delivery candidate. Toxicity assessment is important in predicting whether a bioactive compound may exhibit harmful effects at certain exposure levels while still maintaining therapeutic potential at appropriate dosages. According to Syafrizayanti et al. (2023), toxicity prediction is performed to ensure that candidate compounds possess biological activity without causing excessive toxic effects in living organisms.

In this study, toxicity prediction was carried out using several parameters, including Ames Test, Carcino Mouse, and Carcino Rat. The Ames Test was used to predict the potential mutagenic properties of the ligand complex, whereas Carcino Mouse and Carcino Rat analyses were performed to evaluate the potential carcinogenic effects of the compound in experimental animal models. These parameters provide preliminary information regarding the biosafety and toxicological risk of the proposed drug delivery system. The toxicity prediction results of the ZSM-5–EDTA–rifampicin complex are presented in **Table 6**.

Table 6. Toxicity Prediction Results of the ZSM-5–EDTA–Rifampicin Complex

Compounds	Hepatotoxicity	Carcinogenicity	Mutagenicity	Cytotoxicity	Predicted LD_{50}	Class
Complex of Rifampicin, EDTA and Zeolite ZSM-5	Inactive/ 0.51	Inactive/ 0.58	Active/ 0.56	Inactive/ 0.61	650mg/Kg	5
Rifampicin	Active/ 0.68	Inactive/ 0.51	Inactive/ 0.56	Inactive / 0.58	500mg/Kg	4
ZSM-5	Inactive/ 0.59	Inactive/ 0.59	Inactive/ 0.68	Cytotoxicity / 0.84	300mg/Kg	3

The toxicity prediction results indicated that the ZSM-5–EDTA–rifampicin complex was classified as non-carcinogenic in both mouse and rat models, suggesting that the proposed complex may not possess significant cancer-inducing potential. Interestingly, the complex also showed lower hepatotoxicity potential compared with free rifampicin, indicating that the carrier system may

contribute to reduced toxicological effects. However, the mutagenicity prediction classified the rifampicin complex as active mutagenic, suggesting a potential risk of inducing DNA mutations under certain biological conditions.

Although mutagenicity does not directly indicate carcinogenicity, this finding suggests that further experimental investigations are necessary to comprehensively evaluate the long-term biosafety and toxicological profile of the proposed delivery system. In addition, the higher predicted LD50 value of the rifampicin complex compared with free rifampicin may indicate lower acute toxicity and improved safety tolerance. Overall, these results suggest that the ZSM-5–EDTA–rifampicin system possesses promising characteristics as a controlled drug delivery platform, although further in vitro and in vivo toxicity studies remain essential to confirm its biological safety and therapeutic applicability.

4 Conclusions

Network pharmacology analysis identified CTSK, BCL2, BCL2L1, and MCL1 as potential tuberculosis-related protein targets of rifampicin. Molecular docking showed that both free rifampicin and the ZSM-5–EDTA–rifampicin complex exhibited favorable binding interactions with tuberculosis-associated receptors, particularly against *Mycobacterium tuberculosis*. The proposed interaction model suggested that rifampicin could be retained within the porous EDTA-functionalized ZSM-5 framework through hydrogen bonding and non-covalent interactions, supporting its potential as a controlled drug delivery system. In addition, the semi-realistic DFT-predicted HOMO–LUMO analysis indicated relatively stable electronic properties of the complex with an estimated energy gap of 4.34 eV, suggesting favorable structural stability and adsorption behavior. Toxicity prediction showed that the complex was non-carcinogenic but potentially mutagenic. Overall, these findings suggest that the ZSM-5–EDTA–rifampicin system has potential as a controlled drug delivery candidate for tuberculosis therapy, although further experimental and computational validation is still required.

References

[1] Kayongo A, Nyiro B, Siddharthan T, Kirenga B, Checkley W, Lutaakome Joloba M, et al. Mechanisms of lung damage in tuberculosis: implications for chronic obstructive pulmonary disease. Frontiers in Cellular and Infection Microbiology. 2023;13-2023.

[2] Gai X, Allwood B, Sun Y. Advances in the awareness of tuberculosis-associated chronic obstructive pulmonary disease. Chinese Medical Journal Pulmonary and Critical Care Medicine. 2024;2(4):250–6.

[3] Gulumbe BH, Abdulrahim A, Ahmad SK, Lawan KA, Danlami MB. WHO report signals tuberculosis resurgence: Addressing systemic failures and revamping control strategies. Decoding Infection and Transmission. 2025;3:10004

[4] Farkhan A, Lawpoolsri S, Soonthornworasiri N, Pakasi TT, Sulistyo S, Salsabila A, et al. Spatiotemporal epidemiology, geographic hotspots, and risk factor associations of drug-resistant tuberculosis incidence in Indonesia: a Bayesian hierarchical modelling approach. Infectious diseases of poverty. 2026 Feb;15(1):23.

[5] Baliasa W, Pingkan W, Kaunang J, Harold B, Kairupan R. Hubungan Pengetahuan, Sikap dan Tindakan Penderita Tuberkulosis dengan Hasil Terapi di Puskesmas Biak Banggai. J*ournal of Public Health and Community Medicine*. 2020;1(4):63–9.

[6] Hardie KR, Fenn SJ. JMM profile: Rifampicin: a broad-spectrum antibiotic. *Journal of Medical Microbiology*. 2022;71(8):1–5.

[7] Beebe A, Seaworth B, Patil N. Rifampicin-induced nephrotoxicity in a tuberculosis patient. Journal of clinical tuberculosis and other mycobacterial diseases. 2015 Nov;1:13–5.

[8] Nisrina H, Hilmi IL. Description of Side Effect of Using Antituberculosis Drug in Pulmonary Tuberculosis Patient: Literature Review. *Jurnal eduhealth*. 2022;13(2):684–8.

[9] Hakkimane SS, Gaonkar SL, Shenoy VP, Guru BR. Improving rifampicin stability in the presence of modified isoniazid across different pH environment. Journal of Applied Pharmaceutical Science. 2025;15(12):245–50.

[10] Jayanudin J, Fahrurrozi M, Wirawan SK, Rochmadi. Pengaruh Konsentrasi Larutan Kitosan dan Volume Cross-linker Terhadap Kinetika Release Mikrokapsul Oleoresin Jahe Merah Dalam Medium Simulated Intestinal Fluid (SIF). Eksergi. 2019;16(2):47–52.

[11] Klojdová I, Milota T, Smetanová J, Stathopoulos C. Encapsulation: A Strategy to Deliver Therapeutics and Bioactive Compounds? Pharmaceuticals. 2023;16(3):1–19.
[12] Xu Y, Yan X, Zheng H, Li J, Wu X, Xu J, et al. The application of encapsulation technology in the food Industry: Classifications, recent Advances, and perspectives. Food Chemistry: X. 2024;21:101240.
[13] MacHtakova M, Thérien-Aubin H, Landfester K. Polymer nano-systems for the encapsulation and delivery of active biomacromolecular therapeutic agents. Chemical Society Reviews. 2022;51(1):128–52.
[14] Gao X, Hai X, Baigude H, Guan W, Liu Z. Fabrication of functional hollow microspheres constructed from MOF shells: Promising drug delivery systems with high loading capacity and targeted transport. Scientific Reports. 2016;6(November):1–10.
[15] Andersen A, Chen Y, Birkedal H. Bioinspired Metal – Polyphenol Materials : Self-Healing and Beyond. 2019;
[16] Guo Z, Xiao Y, Wu W, Zhe M, Yu P, Shakya S, et al. Metal–organic framework-based smart stimuli-responsive drug delivery systems for cancer therapy: advances, challenges, and future perspectives. *Journal of Nanobiotechnology*. 2025;23(1). https://doi.org/10.1186/s12951-025-03252-x
[17] Mulyati TA, Pujiono FE. Uji Drug Loading Ibuprofen Pada Material UiO-66 (Zr-Metal Organic Framework). Jurnal Kimia Riset. 2019;4(2):161–9.
[18] Abuçafy MP, Caetano BL, Chiari-Andréo BG, Fonseca-Santos B, do Santos AM, Chorilli M, et al. Supramolecular cyclodextrin-based metal-organic frameworks as efficient carrier for anti-inflammatory drugs. European Journal of Pharmaceutics and Biopharmaceutics. 2018;127(September 2017):112–9.
[19] Hanif QA, Nugraha RE, Lestari WW. Kajian Metal–Organic Frameworks (MOFS) sebagai Material Baru Pengantar Obat. *ALCHEMY Jurnal Penelitian Kimia*. 2018;14(1):16–36.
[20] Li Y, Yu J. New Stories of Zeolite Structures: Their Descriptions, Determinations, Predictions, and Evaluations. Chemical Reviews. 2014 Jul 23;114(14):7268–316. https://doi.org/10.1021/cr500010r
[21] Ishkildina AK, Travkina OS, Serebrennikov D V, Zilberg RA, Malunov AI, Filippova NA, et al. Synthesis of Granular Free-Binder ZSM-5 Zeolites Using Different Amorphous Aluminosilicates. Surfaces. 2025;8(1).
[22] Pandya T, Patel S, Kulkarni M, Singh YR, Khodakiya A, Bhattacharya S, et al. Zeolite-based nanoparticles drug delivery systems in modern pharmaceutical research and environmental remediation. Heliyon. 2024;10(16).
[23] Riwu AAP, Neolaka YAB. Review: Zeolite Alam Sebagai Material Penghantar Obat. Jurnal Beta Kimia. 2021;1(2):7–14.
[24] Al-Thawabeia RA, Hodali HA. Use of Zeolite ZSM-5 for Loading and Release of 5-Fluorouracil. Journal of Chemistry. 2015;2015.
[25] Nurjannah S, Arum D, Syahrani D, Dyanti AP, Sutrisno, Tarigan IL, et al. In Silico Study of Seven Novel Peronemin Compounds from Sungkai Leaves (*Peronema canescens* Jack) as Anti-Inflammatory Linkage Immunomodulatory. Letters in Applied NanoBioScience. 2025;14(3):1–14.
[26] Kim S, Chen J, Cheng T, Gindulyte A, He J, He S, et al. PubChem 2023 update. Nucleic Acids Research. 2023;51(D1):D1373–80.
[27] Palanivel S, Moulishankar A, Murugan S, Kumaradoss KM, Thirugnanasambandam S. Integrated network pharmacology and molecular modeling approaches to reveal the anti-diabetic potential of phytochemicals from Zanthoxylum simulans. Beni-Suef University Journal of Basic and Applied Sciences. 2026;15(1).
[28] Wimalagunasekara SS, Weeraman JWJK, Tirimanne S, Fernando PC. Protein-protein interaction (PPI) network analysis reveals important hub proteins and sub-network modules for root development in rice (Oryza sativa). Journal of Genetic Engineering and Biotechnology. 2023;21(1).https://doi.org/10.1186/s43141-023-00515-8
[29] Sutjiningsih NNO, Ulisya AA, Utami A, Natalia C, Mumtaz FC, Yulanda NRE, et al. Molecular docking of several compounds in

katuk (Sauropus androgynus (L.)) leaves as anti-breast cancer in AKT1 protein. Pharmacy Reports. 2025;4(3):77.

[30] Banerjee P, Eckert AO, Schrey AK, Preissner R. ProTox-II: A webserver for the prediction of toxicity of chemicals. Nucleic Acids Research. 2018;46(W1):W257–63.

[31] Susanto AFS, Jami AS, Muchlisin MA, Almuhtarihan IF. A Network Pharmacology of BrotowalI (Tinospora cordifolia) On Immunity Cases. P*roceedings of International Pharmacy Ulul Albab Conference and Seminar* (PLANAR). 2023;3:29–37.

[32] Gustavo De Oliveira Lasaro L, Nithael F, Lucio M, Silva Marinho E. In Silico Studies of Aurantiamide Acetate: Conformational Characterization and Admet. International *Journal of Recent Research and Review.* 2020;XIII(1):27–38.

[33] Kanagavalli U, Deboral E, Lakshmipriya MD, Sadiq AM, Priya AM. In silico Molecular Docking of Anthraquinone Identified from Boerhavia diffusa Linn against Bax and Bcl-2 Gene. *Journal of Pharmaceutical Research Internationa*l. 2021;33(57A):352–9.

[34] Galla MS, Kale NB, Sharma A, Hajare A, Godugu C, Shankaraiah N. Development of chromone-thiazolidine-2,4-dione Knoevenagel conjugates as apoptosis inducing agents. *Bioorganic and Medicinal Chemistry Letters.* 2024;109:1–8.

[35] Lozano ML, Segú-Vergés C, Coma M, Álvarez-Roman MT, González-Porras JR, Gutiérrez L, et al. Elucidating the mechanism of action of the attributed immunomodulatory role of eltrombopag in primary immune thrombocytopenia: An in silico approach. *International Journal of Molecular Sciences*. 2021;22(13):1–16.

[36] Rahman MF, Kasim A, Djirimu ML, Budiarsa IM. Analisis In-Silico Struktur Tiga Dimensi Reseptor Trk A dan Trk B Protein Neurotrophin 3 Pada Gallus gallus (Chicken). Jurnal Biologi Papua. 2020;12(2):78–84.

[37] Aziz A, Andrianto D, Safithri M. Molecular Docking of Bioactive Compounds from Wungu Leaves (Graptophyllum pictum (L) Griff) as Tyrosinase Inhibitors. Indonesian Journal of Pharmaceutical Science and Technology. 2022;9(2):96–107.

[38]. Lovell SC, Davis, Ian W. Davis 1, Adrendall WB, de Bakker PIW, Word JM, Prisant, Michael G. Prisant 1, et al. Structure validation by c alpha geometry: phi, psi and c beta deviation. Proteins-Structure Function and Genetics. 2003;50(August 2002):437–50.

[39] Malleshappa Gowder S, Chatterjee J, Chaudhuri T, Paul K. Prediction and analysis of surface hydrophobic residues in tertiary structure of proteins. *The Scientific World Journal*. 2014;2014.

[40] Listyani TA, Herowati R. Analisis Docking Molekuler Senyawa Derivat Phthalimide sebagai Inhibitor Non-Nukleosida HIV-1 Reverse Transcriptase. *Jurnal Farmasi Indonesia*. 2018;15(2):123–34.

[41] Liu W, Wu J, Jiang Z, Zhang X, Wang Z, Meng F, et al. Application of Ordered Porous Silica Materials in Drug Delivery: A Review. *Molecules*. 2024;29(23).

[42] Souza IMS, García-Villén F, Viseras C, Perger SBC. Zeolites as Ingredients of Medicinal Products. *Pharmaceutics*. 2023;15(5):1–33.

[43] Syafrizayanti S, Putri A, Salim M, Kusnanda AJ. Simulasi Inhibisi Aktivitas Enzim α-Amilase dan α-Glukosidase oleh Senyawa Bioaktif Mikroalga Spirulina platensis. *ALCHEMY Jurnal Penelitian Kimia*. 2023;19(2):223–33.